

# Thermodynamic description of the competition between quantum dots and quantum dashes during metalorganic vapor phase epitaxy in the InAs/InP(001) system: Experiment and theory

G. Saint-Girons,\* A. Michon, I. Sagnes, G. Beaudoin, and G. Patriarche

*Laboratoire de Photonique et de Nanostructures, LPN/UPR 20-CNRS, Route de Nozay, 91460 Marcoussis, France*

(Received 27 March 2006; revised manuscript received 7 July 2006; published 7 December 2006)

This work reports on the competition between the formation of faceted quantum dots (QDs) and step-bunched quantum sticks (QS) during the metalorganic vapor phase epitaxy of InAs on InP(001). QS are formed under low V/III ratios ( $<10$ ), while higher V/III ratios enhance the formation of QD. These results are analyzed using a model proposed by Tersoff *et al.* The good correlation between theory and experiment supports our conclusion that thermodynamics play a determinant role in the transition from QS to QD, and that this transition is related to an increased QD facet energy at high V/III ratios.

DOI: [10.1103/PhysRevB.74.245305](https://doi.org/10.1103/PhysRevB.74.245305)

PACS number(s): 81.07.Ta, 81.05.Ea, 81.10.-h, 81.15.Gh

## I. INTRODUCTION

The singular physical properties of self-assembled InAs/InP nanostructures have motivated numerous studies in various research fields since their first fabrication in 1991.<sup>1</sup> The causes of these infatuation partly rely in the emission wavelength of these nanostructures that can be tuned to 1.55  $\mu\text{m}$ . This wavelength range is of particular interest for various applications such as low threshold laser sources for long-haul telecommunications<sup>2</sup> or single photon emitters for quantum cryptography systems.<sup>3</sup> Molecular beam epitaxy (MBE), chemical beam epitaxy (CBE), and metalorganic vapor phase epitaxy (MOVPE) have been used to fabricate InAs/InP nanostructures in the Stranski-Krastanov (SK) growth mode. These studies indicate that the deposition of InAs on InP(001) in standard SK MBE growth conditions leads to the formation of quantum sticks (QS) or quantum wires (QWr), more or less strongly elongated along the  $[1-10]$  crystallographic direction.<sup>4,5</sup> Some works show that three-dimensional quantum dots (QDs) can be obtained by MBE by depositing InAs on (311)B oriented substrates,<sup>6</sup> on InAlAs buffers grown on InP(001) substrates,<sup>7</sup> on corrugated or misoriented InP surfaces,<sup>5</sup> or under high As partial pressures.<sup>8</sup> On the opposite, no observation of MOVPE grown InAs/InP QS or QWr has to the best of our knowledge been reported yet. The standard SK MOVPE growth conditions lead to the formation of quantum dots (QD) in this material system.<sup>9,10</sup> Regarding CBE, both QD and QS have been fabricated, depending on the growth conditions.<sup>11,12</sup> The fundamental mechanisms promoting the formation of QD or QWr remain unclear, as illustrated by the discrepancy of the experimental results reported in the literature. In Ref. 13, the authors theoretically show that above a critical size, it becomes energetically favorable for QD having an initial isotropic shape to elongate, leading to the formation of QS-like nanostructures. These calculations, supported by subsequent experimental works,<sup>14</sup> predict a transition from isotropic QD to elongated nanostructures increasing the amount of deposited material. However, they do not elucidate the reasons why QWr or QS can be directly formed (in particular by MBE or CBE) without intermediate QD shape. The study reported in this work demonstrate that either QD or QS can be formed by MOCVD by depositing

InAs on InP(001) in the SK growth mode. QS are obtained at low V/III ratios, while QD are formed under high V/III ratios. The structural properties of the nanostructures are analyzed by adapting the model proposed in Ref. 13. These calculations, strongly supported by our experimental results, show that the reduction of the V/III ratio during the growth of InAs on InP(001) leads to a decrease of the facet energy of the QD, thus promoting the formation of step-bunched QS under As-poor conditions.

## II. GROWTH OF THE SAMPLES

The samples studied in the following were grown at a pressure of 60 Torr in a MOVPE system using hydrogen as carrier gas. Standard precursors [arsine, phosphine, and trimethylindium (TMI)] were used. The growth sequence is as follows: after a 150 nm thick InP buffer layer deposited at 625  $^{\circ}\text{C}$  on exactly (001)-oriented InP substrates, the growth temperature is lowered to 530  $^{\circ}\text{C}$  and 4 monolayers (ML) of InAs are grown, followed by 40 nm of InP. Two series of samples were grown. For the first series, the  $\text{AsH}_3$  flow rate  $F_{\text{As}}$  was kept constant to 6 sccm ( $F_{\text{As}}=4.44 \mu\text{mol s}^{-1}$ ) during the InAs growth, and the TMI flow rate  $F_{\text{In}}$  was set to 0.38, 0.225, 0.152, and 0.036  $\mu\text{mol s}^{-1}$  for samples In<sub>1</sub>, In<sub>2</sub>, In<sub>3</sub>, and In<sub>4</sub>, respectively. For the second series,  $F_{\text{In}}$  was kept constant to 0.38  $\mu\text{mol s}^{-1}$ , and  $F_{\text{As}}$  was set to 7.4, 3.3, and 1.6  $\mu\text{mol s}^{-1}$  for samples As<sub>1</sub>, As<sub>2</sub>, and As<sub>3</sub>, respectively. In the following, the V/III ratio ( $F_{\text{As}}/F_{\text{In}}$ ) used for the growth of InAs will be referred to as  $R$ .

## III. EXPERIMENTAL EVIDENCE OF A TRANSITION FROM FACETTED QD TO STEP-BUNCHED QS

Transmission electron microscope (TEM) plane views of samples In<sub>1</sub> and As<sub>3</sub> are shown in Fig. 1. The geometry of the QD has already been described elsewhere.<sup>15</sup> Sample In1 ( $R=11.7$ ) contains well-defined parallelogram-shaped QD with edges oriented along the  $[1-30]$  and  $[3-10]$  directions. Some QD are diamond-shaped, but most of them are slightly elongated, either in the  $[1-30]$  or in the  $[3-10]$  direction. The QD density is approximately  $2.5 \times 10^{10} \text{ cm}^{-2}$ . In the following, the “widths” of the parallelograms perpendicular to the  $[1-30]$  (respectively  $[3-10]$ ) direction will be referred to as

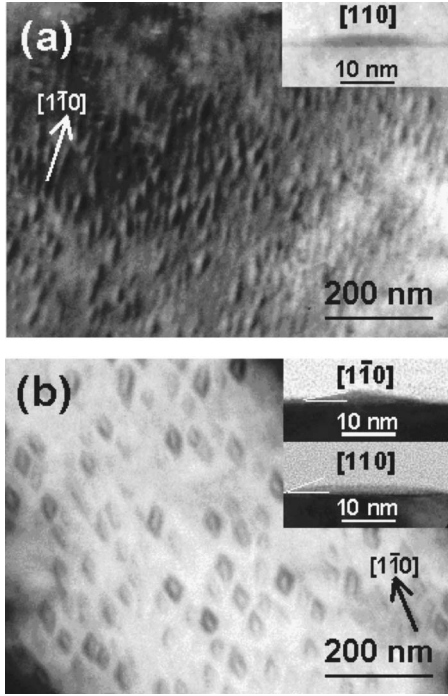


FIG. 1. (a) TEM plane view of sample  $As_3$  taken under 220 dark field conditions. Inset, TEM cross-sectional view of a QS. (b) TEM plane view of sample  $In_1$  taken under 001 bright field conditions. Inset, cross-sectional views of a QD (sample cleaved along the  $[110]$  and  $[1-10]$  directions).

$W_1$  (respectively,  $W_2$ ). For each QD, the smallest (respectively, largest) width of the parallelogram will be referred to as  $W_{\min}$  (respectively,  $W_{\max}$ ). The average value of  $W_{\min}$  (respectively,  $W_{\max}$ ) is 19.1 nm (respectively, 27.1 nm), as extracted from a statistical analysis over about 100 QD. Typical TEM cross-sectional views of the QD of an uncapped sample equivalent to sample  $In_1$  are shown in the inset of Fig. 1(b). The QD is clearly faceted, the angle between the (001) growth surface and the QD facet being approximately  $25.2^\circ$  in the  $(1-10)$  plane and  $13.3^\circ$  in the  $(110)$  plane. These angles correspond to  $\{136\}$  facet planes, as shown in Ref. 15 and as already observed in Refs. 16 and 17. In this QD geometry, the height  $h$  of a particular QD (excluding the wetting layer) is related to its lateral dimension  $W_{\min}$ ,

$$h = 0.2635W_{\min}. \quad (1)$$

The value of  $h$ , calculated using  $W_{\min} = 19.1$  nm, is 5.0 nm in good agreement with atomic force microscopy measurements (not shown here). Similar QD were observed in samples  $In_2$  ( $R = 19.7$ ),  $In_3$  ( $R = 29.2$ ),  $In_4$  ( $R = 122.3$ ), and  $As_1$  ( $R = 19.5$ ).

The nanostructures of samples  $As_2$  and  $As_3$  ( $R = 8.7$  and 4.2, respectively) strongly differ from the ones of the other samples. A typical TEM plane view of sample  $As_3$  taken under 002 dark field conditions is shown in Fig. 1(a) (similar morphology was observed for sample  $As_2$ ). The sample contains QS, elongated along the  $[1-10]$  direction. Their density is about  $10^{11} \text{ cm}^{-2}$ , and their average length (respectively, width) is 19.5 nm (respectively, 82.1 nm). The ratio length/

width is in average 4.2, that is 3 times larger than the ratio  $W_{\max}/W_{\min}$  of the QD of sample  $In_1$ . The contrast of these QS is very weak under 001 zone-axis bright field conditions (not shown here). This observation, as well as the cross-sectional view shown in the inset of Fig. 1(a), strongly suggests that the QS are not faceted, but formed by an accumulation of atomic steps. The average height of the QS measured on TEM cross-sectional views is 1 nm (excluding the wetting layer).

The morphological study presented above shows that below a critical value  $R_c^{\text{exp}}$  of the V/III ratio verifying  $8.7 < R_c^{\text{exp}} < 11.7$ , the deposition of InAs on InP in our growth conditions leads to the formation of step-bunched QS instead of faceted QD. A detailed analysis of this phenomenon is carried out in the following.

#### IV. THERMODYNAMIC INTERPRETATION

The model proposed in Ref. 13 was adapted to our QD geometry to calculate their energy of formation. Similar thermodynamic treatment has already been described in Ref. 15. The formation energy of a single QD is then given by

$$\Delta E = \Delta E_{\text{surf}} + \Delta E_{\text{el}}, \quad (2)$$

where  $\Delta E_{\text{surf}}$  is the excess of surface energy due to the formation of a single QD, and  $\Delta E_{\text{el}}$  is the amount of elastic energy relaxed by the formation of a QD. Taking into account our QD geometry,  $\Delta E$  is given by

$$\Delta E = \Gamma W_1 W_2 - 2ch^2 \left[ \frac{W_1}{\sin(\phi)} \ln \left( \frac{W_2}{h \cotan(\theta)} e^{1.5} \right) + \frac{W_2}{\sin(\phi)} \times \ln \left( \frac{W_1}{h \cotan(\theta)} e^{1.5} \right) \right], \quad (3)$$

where

$$c = \left( Y_M \frac{\Delta a}{a} \right)^2 \frac{1 - \nu}{2\pi\mu}, \quad (4)$$

$\Delta a/a = 0.032$  is the lattice mismatch between InAs and InP, and  $Y_M = 5.14 \times 10^{10} \text{ Pa}$ ,  $\mu = 2.25 \times 10^{10} \text{ Pa}$ , and  $\nu = 0.39$  are the Young's modulus, the shear modulus of InAs, and the Poisson ratio of InAs, respectively.  $\phi = 53.1^\circ$  is the angle between two subsequent edges of the QD,  $\theta = 27.8^\circ$  is the angle between the (001) plane and the  $\{136\}$  facets of the QD, and  $\Gamma = 1.4138 \times \gamma_{136} - 1.2505 \times \gamma_{001}$ , where  $\gamma_{136}$  (respectively,  $\gamma_{001}$ ) are the surface energies of the (001) [respectively, (136)] planes. In the following, the problem will be treated by considering that the height  $h$  of the QD is constant and equal to its average experimental value for each sample. In fact, the model of Ref. 13 is not suited for the analysis of the variation of  $\Delta E$  with respect to  $h$ , since the authors assume that the strain within the island does not vary in the  $z$  direction. This approximation, reasonable in the case where the height of the QD is much smaller than their lateral dimensions (which is the case for our QD), allows to reach an analytical formulation of  $\Delta E$  as a function of  $W_1$  and  $W_2$  but

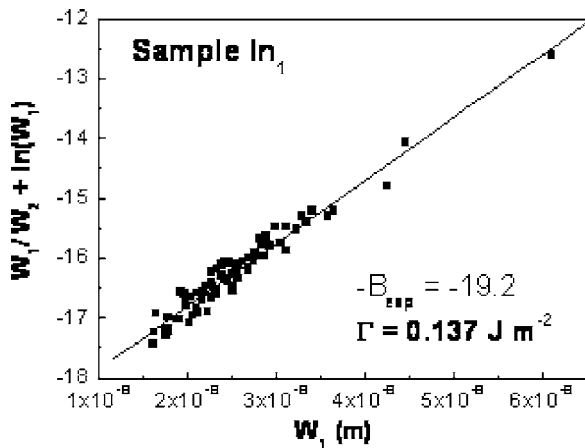


FIG. 2. Variation of  $W_1/W_2 + \ln(W_1)$  as a function of  $W_1$  for sample In1. Square, experimental values extracted from Fig. 1(b) and continuous line, linear regression of the experimental data. The value of  $\Gamma$  extracted from the linear regression is  $0.137 \text{ J m}^{-2}$ .

leads to an imprecise description of the variation of  $\Delta E$  with  $h$ . Minimizing  $\Delta E$  with respect to  $W_2$  keeping  $h$  constant leads to

$$\frac{W_1}{W_2} + \ln W_1 = \frac{\Gamma W_1}{A h^2} - B, \quad (5)$$

where  $A = \frac{2c}{\sin \varphi}$  and  $B = \ln \frac{e^{1.5}}{\sin \varphi \times \cotan \theta}$ . The experimental variation of  $\frac{W_1}{W_2} + \ln W_1$  with  $W_1$  is plotted in Fig. 2 for sample In1, as deduced from the TEM plane view of Fig. 1(b).  $\frac{W_1}{W_2} + \ln W_1$  increases linearly with  $W_1$ , as predicted by Eq. (5). This shows that despite the fact that  $h$  is kept constant in the analysis presented here, the model proposed in Ref. 13 adapted to our QD geometry describes very well the geometry of our QD. In particular, the elongation of the QD along [1-30] or [3-10] appears to be driven by thermodynamics, and results in a minimization of  $\Delta E$  for each value of  $W_1$  (see Ref. 15). Note that the QD geometry described by Eq. (5) does not correspond to an absolute minimum of  $\Delta E$ . In fact minimizing  $\Delta E$  with respect to  $W_1$  and  $W_2$  leads to an optimal diamond-shape configuration defined by

$$W_1 = W_2 = W = \frac{\Gamma}{\varepsilon_1(1 + \varepsilon_2)}, \quad (6)$$

where  $\varepsilon_1 = A \times 0.2635^2$  and  $\varepsilon_2 = B - \ln(0.2635)$ . The value of  $\Gamma$ , extracted from the linear regression of Fig. 2, is  $0.137 \text{ J m}^{-2}$  for sample In1. Similar treatments were performed for samples In2, In3, In4, and As1. Very good agreements between experiment and theory were found for all samples. The values of  $\Gamma$  obtained from this analysis are plotted as a function of the V/III ratio  $R$  in Fig. 3.  $\Gamma$  appears to increase linearly with  $R$ . A linear regression of the experimental data of Fig. 3 leads to

$$\Gamma(R) \approx 0.12 + 0.00138 \times R. \quad (7)$$

We attribute this increase to a variation of the dimerization rate of the QD facet depending on the concentration of As species in the gas phase.<sup>18</sup> The increase of  $\Gamma$  increasing  $R$  has

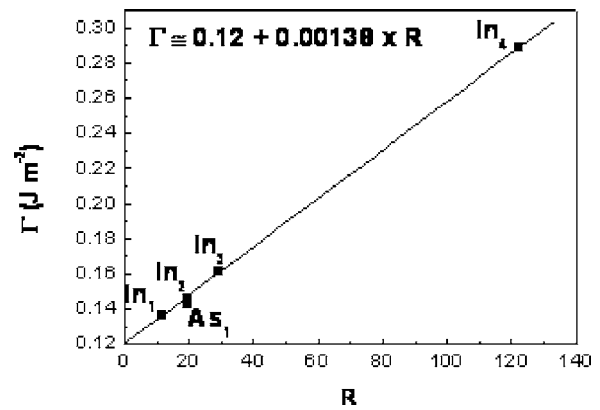


FIG. 3. Variation of  $\Gamma$  as a function of the V/III ratio  $R$  and its linear regression (continuous line).

a strong influence on the formation energy of the QD [Eq. (3)]. The formalism described above allows to determine the formation energy  $\Delta E_{\text{eq}}$  of an equilibrium-shaped QD, by combining Eqs. (3), (6), and (7):

$$\Delta E_{\text{eq}} = \frac{\Gamma(R)^2}{\varepsilon_1^2(1 + \varepsilon_2)^2} - \frac{2\varepsilon_1\Gamma(R)^2}{\varepsilon_1^2(1 + \varepsilon_2)^2} \left[ \varepsilon_2 + \ln \left( \frac{\Gamma(R)}{\varepsilon_1(1 + \varepsilon_2)} \right) \right] \times \left( \frac{\Gamma(R)}{\varepsilon_1(1 + \varepsilon_2)} - 1 \right). \quad (8)$$

The evolution of  $\Delta E_{\text{eq}}$  as a function of  $R$  is plotted in Fig. 4.  $\Delta E_{\text{eq}}$  decreases increasing  $R$  due to the increase of  $\Gamma$ .

The same model was used to calculate the formation energy  $\Delta E_{\text{QS}}$  of a QS from sample As2 or As3. An important number of QS samples grown in various conditions have been analyzed by TEM. These analyses show that the width (smallest lateral dimension) and the height of the QS are similar in all these samples and do not strongly depend on the growth conditions. Average widths (respectively, heights) of  $19.5 \pm 2 \text{ nm}$  (respectively,  $1 \pm 0.1 \text{ nm}$ ) were measured for all the samples. The length of the QS, which mainly depends on the growth kinetics (diffusion along [1-10]) varies with the growth conditions. From a general point of view, growth conditions that enhance diffusion (low growth rate of high

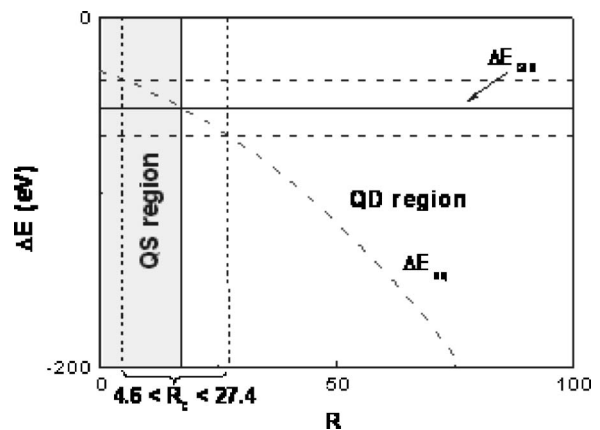


FIG. 4. Formation energy of a single QD (dashed line) and a single QS (continuous line) as a function of  $R$ .

growth temperature) systematically lead to increased QS lengths as compared to growth conditions where adatoms diffusion is inhibited. The amount of elastic energy relaxed by the formation of a single QS was calculated using the methodology presented above, and the term corresponding to the variation of the surface energy was calculated by considering the QS as an accumulation of surface steps.  $\Delta E_{\text{QS}}$  is therefore given by

$$\begin{aligned} \Delta E_{\text{QS}} = & \frac{2h_{\text{QS}}}{a_p} (L_{\text{QS}}\lambda_{1-10} + W_{\text{QS}}\lambda_{110}) \\ & - 2ch_{\text{QS}}^2 \left[ L_{\text{QS}} \ln \left( \frac{W_{\text{QS}}e^{1.5}}{h_{\text{QS}} \cot \text{an}(\theta_{\text{QS}})} \right) \right. \\ & \left. + W_{\text{QS}} \ln \left( \frac{L_{\text{QS}}e^{1.5}}{h_{\text{QS}} \cot \text{an}(\theta_{\text{QS}})} \right) \right], \end{aligned} \quad (9)$$

where  $h_{\text{QS}}$  (respectively  $L_{\text{QS}}$  and  $W_{\text{QS}}$ ) are the height (respectively, length and width) of the QS,  $a_p$  is the perpendicular lattice parameter of InAs uniformly strained on InP,  $2h_{\text{QS}}/a_p$  is the number of atomic steps that compose the QS,  $\theta_{\text{QS}} = \arctan\left(\frac{h_{\text{QS}}}{L_{\text{QS}}/2}\right)$  is the angle between the side of the QS and the surface, and  $\lambda_{1-10}$  (respectively,  $\lambda_{110}$ ) is the energy of step creation along  $[1-10]$  (respectively,  $[110]$ ) for the InAs(001) surface. Based on our observation that  $W_{\text{QS}}$  and  $h_{\text{QS}}$  does not depend on the growth conditions in the entire range explored,  $\Delta E_{\text{QS}}$  was calculated using the average values of the QS dimensions,  $W_{\text{QS}} = 19.5 \pm 2$  nm and  $h_{\text{QS}} = 1 \pm 0.1$  nm. An error bar was also calculated for  $\Delta E_{\text{QS}}$ , in order to take into account the dispersions of  $W_{\text{QS}}$  and  $h_{\text{QS}}$  for the different samples. Moreover, a careful study of  $\Delta E_{\text{QS}}$  as defined by Eq. (9) shows that the dependence of  $\Delta E_{\text{QS}}$  with  $L_{\text{QS}}$  is very small. This is due to the fact that  $\lambda_{1-10}$  is much smaller than  $\lambda_{110}$  (see below), and that  $L_{\text{QS}}$  is the largest dimension of the QS, which leads to a poor efficiency of the elastic energy relaxation along  $[1-10]$ . The value of  $L_{\text{QS}}$  that we used for the calculation is therefore the one corresponding to sample As<sub>3</sub>, namely  $L_{\text{QS}} = 82.1$  nm. The energy of step creation are to the best of our knowledge not referenced in the literature for InAs surfaces. In Ref. 19, values are derived for a  $(2 \times 4)$  reconstructed (001) GaAs surface,  $\lambda_{1-10}(\text{GaAs}) = (2.7 \pm 1.3) \times 10^{-12}$  J m<sup>-1</sup> and  $\lambda_{110}(\text{GaAs}) = (1.6 \pm 0.25) \times 10^{-11} \pm 0.25$  J m<sup>-1</sup>. For an InAs surface, the energies of step creation are smaller, because the InAs surface bond strength is smaller than the one of GaAs. The surface bond strengths of several III-V compounds are experimentally determined in Ref. 20. Values of 233 (respectively, 149) kJ mol<sup>-1</sup> are found for (001)-oriented GaAs (respectively, InAs) surfaces. To estimate the

energies of step creation for InAs, the values of Ref. 19 were weighted by the surface bond strengths. We thus considered  $\lambda_{1-10}(\text{InAs}) = (1.7 \pm 0.8) \times 10^{-12}$  J m<sup>-1</sup> and  $\lambda_{110}(\text{InAs}) = (1.0 \pm 0.25) \times 10^{-11}$  J m<sup>-1</sup> for our calculation. We also considered that  $\lambda_{1-10}(\text{InAs})$  and  $\lambda_{110}(\text{InAs})$  does not depend on  $R$ . This hypothesis relies on the fact that the InAs surface reconstruction does not vary in the entire range of  $R$  considered in this study. Taking into account the uncertainty on  $\lambda_{1-10}(\text{InAs})$  and  $\lambda_{110}(\text{InAs})$  as well as the dispersion of  $W_{\text{QS}}$  and  $h_{\text{QS}}$ , we found  $\Delta E_{\text{QS}} \approx -51.4 \pm 16.3$  eV. The variations of  $\Delta E_{\text{QS}}$  and  $\Delta E_{\text{eq}}$  with  $R$  are compared in Fig. 4. Below a critical value of  $R$  referred to as  $R_c$ ,  $\Delta E_{\text{QS}}$  becomes smaller than  $\Delta E_{\text{eq}}$ . This indicates that for  $R < R_c$ , the formation of QS leads a more efficient reduction of the total energy of the system than the formation of QD. For  $R > R_c$ , QD becomes thermodynamically more stable than QS. The value of  $R_c$  extracted from Fig. 4 is so that  $4.6 < R_c < 27.4$ . This calculation matches the experimental results discussed above: the experimental value  $R_c^{\text{exp}}$  of the V/III ratio for which a transition from QS to QD is observed is so that  $8.7 < R_c^{\text{exp}} < 11.7$ .

## V. CONCLUSION

Our calculations, only based on thermodynamic considerations and strongly supported by our experimental observations, show that the formation of QD is enhanced under As-rich growth conditions, due to an increase of their facet energy. This result shows that apart from the growth kinetics, thermodynamics play an important role in the formation of QS or QD during the SK growth of InAs on InP(001) substrate. This conclusion is consistent with the experimental results reported in the literature: MBE growth conditions, characterized by relatively low As partial pressures, enhance the formation of QS while CBE or MOVPE growth conditions enhance the formation of QD. In the end, this work opens the way to a better control of the MOVPE growth of InAs/InP nanostructures. The use of the model proposed in Ref. 13 could be extended to study the influence of other growth parameters on their size, shape, and density. In particular, a more precise knowledge of their formation process could be achieved by analyzing the influence of the amount of InAs deposited to form the QD on the basis of this model.

## ACKNOWLEDGMENTS

The authors gratefully thank Frank Glas for useful discussions. This work was supported by the SANDIE EC Network of Excellence, by SESAME Contract No. 1377, by the Région Ile de France, and by the Conseil Général de l'Essonne.

\*Corresponding author. Electronic address: guillaume.saint-girons@ec-lyon.fr

<sup>1</sup>J. F. Carlin, R. Houdré, A. Rudra, and M. Illegems, Appl. Phys. Lett. **59**, 3018 (1991).

<sup>2</sup>D. Hadass, R. Alizon, H. Dery, V. Mikhelashvili, G. Eisenstein,

R. Schwertberger, A. Somers, J. P. Reithmaier, A. Forchel, M. Calligaro, S. Bansropun, and M. Krakowski, Appl. Phys. Lett. **85**, 5505 (2004).

<sup>3</sup>K. Takemoto, Y. Sakuma, S. Hirose, T. Usuki, and N. Yokoyama, Jpn. J. Appl. Phys., Part 2 **43**, L349 (2004).

- <sup>4</sup>M. Gendry, C. Monat, J. Brault, P. Regreny, G. Hollinger, B. Salem, G. Guillot, T. Benyattou, C. Bru-chevallier, G. Bremond, and O. Marty, *J. Appl. Phys.* **95**, 4761 (2004).
- <sup>5</sup>L. González, J. M. García, R. García, F. Briones, J. Martínez-Pastor, and C. Ballesteros, *Appl. Phys. Lett.* **76**, 1104 (2000).
- <sup>6</sup>C. Paranthoen, N. Bertru, O. Dehaese, A. Le Corre, S. Loualiche, B. Lambert, and G. Patriarche, *Appl. Phys. Lett.* **78**, 1751 (2001).
- <sup>7</sup>J. Brault, M. Gendry, G. Grenet, G. Hollinger, J. Olivares, B. Salem, T. Benyattou, and G. Bremond, *J. Appl. Phys.* **92**, 506 (2002).
- <sup>8</sup>H. J. Parry, M. J. Ashwin, J. H. Neave, and T. S. Jones, *J. Cryst. Growth* **278**, 131 (2005).
- <sup>9</sup>K. Kawaguchi, M. Ekawa, A. Kuramata, T. Akiyama, H. Ebe, and M. Sugawara, *Appl. Phys. Lett.* **85**, 4331 (2004).
- <sup>10</sup>A. Michon, G. Saint-Girons, G. Beaudoin, I. Sagnes, L. Largeau, and G. Patriarche, *Appl. Phys. Lett.* **87**, 253114 (2005).
- <sup>11</sup>H. R. Gutiérrez, M. A. Cotta, and M. M. G. de Carvalho, *Appl. Phys. Lett.* **79**, 3854 (2001).
- <sup>12</sup>Q. Gong, R. Nötzel, P. J. van Veldhoven, T. J. Eijkemans, and J. H. Wolter, *Appl. Phys. Lett.* **84**, 275 (2004).
- <sup>13</sup>J. Tersoff and R. M. Tromp, *Phys. Rev. Lett.* **70**, 2782 (1993).
- <sup>14</sup>Q. Gong, R. Nötzel, P. J. van Veldhoven, T. J. Eijkemans, and J. H. Wolter, *J. Cryst. Growth* **280**, 413 (2005).
- <sup>15</sup>A. Michon, I. Sagnes, G. Patriarche, G. Beaudoin, M. N. Mérat-Combes, and G. Saint-Girons, *Phys. Rev. B* **73**, 165321 (2006).
- <sup>16</sup>T. Hanada, B. H. Koo, H. Totsuka, and T. Yao, *Phys. Rev. B* **64**, 165307 (2001).
- <sup>17</sup>H. Hwang, S. Yoon, H. Kwon, E. Yoon, H. Kim, J. Y. Lee, and B. Cho, *Appl. Phys. Lett.* **85**, 6383 (2004).
- <sup>18</sup>E. Pehlke, N. Moll, A. Kley, and M. Scheffler, *Appl. Phys. A: Mater. Sci. Process.* **A65**, 525 (1997).
- <sup>19</sup>E. J. Heller, Z. Y. Zhang, and M. G. Lagally, *Phys. Rev. Lett.* **71**, 743 (1993).
- <sup>20</sup>O. Féron, Y. Nakano, and Y. Shimogaki, *J. Cryst. Growth* **221**, 129 (2000).